Solar Energy Simulation of Bifacial Panels for Performance Optimisation

Ernest Sng
Univeristy of Glasgow
Glasgow, United Kingdom
ernest.sng@recgroup.com

Sai Wei Chua
Univeristy of Glasgow
Glasgow, United Kingdom
2427488C@student.gla.ac.uk

Scott Roy
Univeristy of Glasgow
Glasgow, United Kingdom
Scott.Roy@glasgow.ac.uk

Idris Lim
Univeristy of Glasgow
Glasgow, United Kingdom
LiHonIdris.Lim@glasgow.ac.uk

***Abstract*— Recent developments on Bifacial Photovoltaic (PV) modules have captured a significant amount of attention as this technology is becoming more affordable and is able to produce more output compared to the traditional monofacial solar panels, the advantage of this technology comes from its ability to absorb additional irradiance from the rear which the monofacial panel is in capable of. Despite being more affordable and able to produce more power, this technology is still not widely used as there is still many issues in predicting the output of the rear accurately through simulations. The rear irradiance is affected by many factors such as the albedo of the ground, reflectivity of the surrounding surfaces, the height from the ground, the tilt angle and the mounting structure.**

Keywords—bifacial modules

I. INTRODUCTION

Solar panels are known to produce electricity when exposed to sunlight. The panel is made up of many solar cells, these solar cells produces electricity when it captures the irradiance of the sunlight, this effect is known as the Photovoltaic effect [1]. The commonly seen panels are the monofacial panels which only collects irradiance from the front surface, the new bifacial PV module collects irradiance from both the front and the rear surface of the module which produces more power compared to the traditional monofacial panels.

Bifacial PV technology was first introduced as a new concept in 1960 to improve the output of PV system. It then quickly leads to the development of the first Bifacial PV cell which can capture irradiance from both the front and the rear simultaneously. This development quickly grew and captured many attentions after a group of researchers from Spain presented results which shows that high efficiency and gain in bifacial PV cells in 1980. Subsequently, it is accepted that Bifacial solar cells can increase the power output of a module compared to the traditional Monofacial solar cells with the implementation of cost-effective solutions at the same time.

The Bifacial PV technology came to be even more aware globally when many companies started to commercialize it in 2010s. A bifacial PV power plant was built in Japan in 2013, an increased gain of 21.9% was observed when compared to a traditional monofacial power plant of similar size even though the installation was sub-optimal [2]. Modelling and simulation are commonly used to analyze the performance of the module, the front surface of the bifacial module is simulated the same way as the front surface of monofacial module. The rear surface of the module, however, is simulated along with many different factors such as the mounting structure, the albedo of the ground and the reflectance of the surroundings which differs from location to location. These factors become the challenges in predicting the rear irradiance accurately [3].

Ray Tracing is technique which can trace the path of light and accurately simulate the way light bounce off an object. Compared to View Factor, Ray Tracing is much harder to use and implement due to the amount of effort required but can simulate results that View Factor cannot. Like View Factor, Ray Tracing is also widely used to simulate Monofacial module, it is mostly used when geometry is irregular and mounting structure and in place and can produce accurate results where View Factor becomes complex to use when dealing with irregular geometry. Although Ray Tracing is more accurate when compared to View Factor, it is very resource demanding and would require a lot of time and effort to produce results for large scale simulation. In addition, Ray Tracing can also be used to find the efficiency of the design of the module [4].

View Factor method is used to create a 2D model to simulate the front and rear irradiance of the Bifacial module while taking into consideration for the reflections from its surroundings [5]. The presented model can give a similar trend to the measured data and predict accurate results only at specific times. The experiment only tested the modules in 0˚ and 30˚ at fixed height which does not give a relation between different configurations and the gain produced. Similar works have also been done by other researchers to predict the gain at both side of the module at different rows but using View Factor and Ray Tracing [5]. A 3x3 PV system was tested at different tilt angle and height separately. The different configurations were then simulated by 3 different models created which models the front and the rear differently. The work showed that increasing height of the module would yield higher gain until a saturation point where the gain will no longer increase despite increasing the height of the module, accurate prediction of rear gains up to 45˚ was also obtainable in through the model.

Reported works from other researchers on the front irradiance of bifacial module, using Ray Tracing has proven to be accurate with different inter-cell gap and is even able to calculate the additional contribution of rays that are being reflected back to the cell by a reflective layer in different position of the module [6]. These works presented accurate models for simulating different design of the Bifacial modules but without any tilting and ground effect. Another work presented by another group of researchers showed that tilt angle is important in Bifacial module performance optimization, they

investigated in the minimum and maximum amount of rays that would affect the module with respect to different tilt angle[7].

The rear irradiance is a challenge to measure as it affected various factors such as the albedo of the ground, reflectivity of the nearby surroundings, material of the module, height of module from the ground and tilt angle [8].

Various work has been done by a group of researchers to calculate the rear irradiance of Bifacial modules [9]. The rear irradiance was modelled using cell level View Factor and Ray Tracing at fixed tilt angle. Results generated from the 2 model was proven to be follow the trend of the measured ISC very well. It is concluded that Ray Tracing is more suitable for more detailed areas like module design and optimization while View Factor is more suitable for simulating array performance. In [10], only cell level View Factor is used to model the rear irradiance of the module at same configuration as the simulation results obtained by the model is shown to differ by roughly ±10% when compared to the measured irradiance.

So far, there are few works done with Ray Tracing on the rear-side of the Bifacial module with respect to different tilt angle and height for performance optimization [11]. This project is built upon the reported works, with the objective of obtaining the optimal performance of the module with only the rear gain using Ray Tracing with respect to different tilt angle and height, which relates to real-world configurations where different area requires different configuration.

The remaining part of this paper is sectioned as: Section 2 presents the system overviews and the methods used for the modelling and simulation. Results of the simulation were discussed in Chapter 3. Conclusions are presented in Section 4.

II. Methodology of Simulation

A. Equations

In this simulation, the point of origin is set to be in the middle of the module, along the plane where the cells lie. The first step is to create a middle plane where all cell lies on so the whole module can be created by referencing from the middle plane. Since the point of origin is set in the middle of the plane, the plane is created using Equation (1), (2) and (3). The plane is set in a view perspective where the breadth of the is on the x-z axis and length is on the y-z axis. The module is mounted in landscape manner such that it mimics the configuration in real-world, the tilting of the module will only apply on the x-z plane so it is assumed that the tilt will have no effect on the y-axis.

$$x = \pm \frac{1}{2} breadth.cos(\theta) \quad (1)$$

$$z = \pm \frac{1}{2} breadth.sin(\theta) \quad (2)$$

$$y = \pm \frac{1}{2} length \quad (3)$$

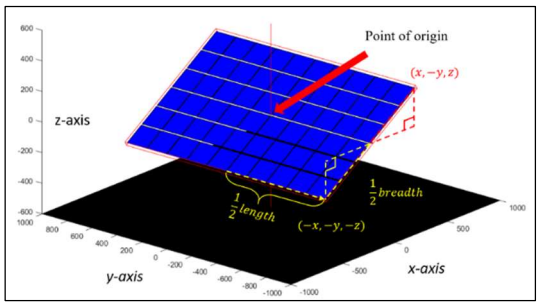

Figure 1. 3D model of module.

The coordinates of the 4 corners of the cells are calculated using equation (4) to (9). The module consists of 60 cells. The cells are categorized into 6 rows and 10 columns. To locate where the 60 cells will be situated in the middle plane, every corner of the cell must be calculated, the calculations of the cells are done in 2 different 2D view, x-z plane and y-z plane. The corners of the cells are labelled as "cell start" and "cell end" in each 2D view. The corners of the middle plane are numbered 1 to 4. Corner 1 of the plane is used as a starting point (sp) to calculate the coordinates of the 4 corners of the 60 cells.

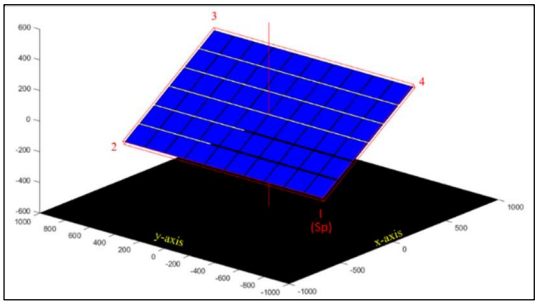

Figure 2. Labelling of the corner of the module.

The basic calculation of the coordinates of the 1800 outgoing scattered rays can be calculated using equation (10) and (11) [18]. This equation requires the coordinates of the point of incidence (x_1) and the height, which is the distance between the highest point of the module and the ground. The height in this formula is assumed to be the large so that the reflected rays will pass through the module to be able to find the intersection point later.

$$x_2 = x_1 + height.tan(\theta)\, cos\,(\varphi) \quad (10)$$

$$y_2 = y_1 + height.tan(\theta)\, sin\,(\varphi) \quad (11)$$

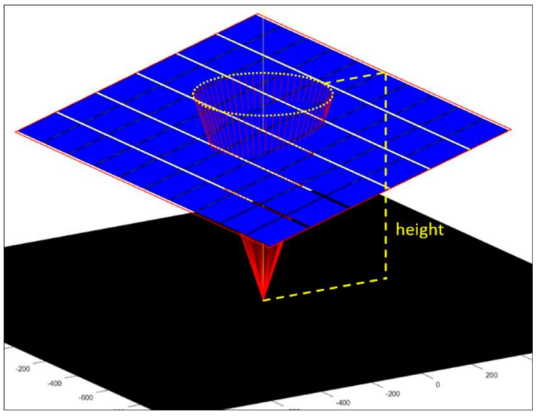

Figure 4. Scattering of rays in 1 polar angle only

After obtaining the final coordinates of the rays, each ray will be turned into a vector, which is used to calculate the intersection point of the ray and the module using dot product. the starting point and the ending point of the reflected ray is defined as P_0 and P_1. The direction of the reflected ray can be defined as u = P_1-P_0. The equation of the line can be represented as P(s)=P_0+su. Where s is a fraction on the line vector P_1 P_0. The normal of the plane, n is defined as the cross product of 2 vectors that lies on the plane. The dot product of 2 vectors perpendicular to each other is 0, this property will be used to find the intersection point of the ray and the plane [12].

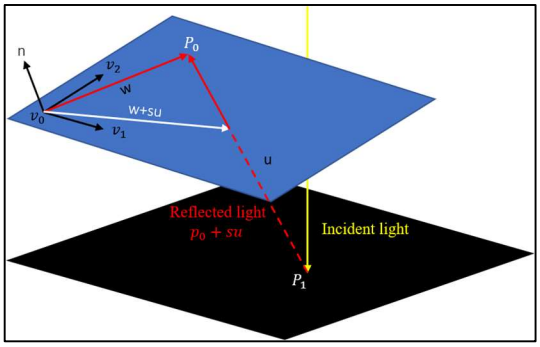

Figure 5. Vector representation of plane-line intersection

The intersection point lies on the plane itself and on a certain point on the vector u which is assumed as su, therefore the dot product of the normal of the plane and the vector from v_0 to the point where to ray intersects the plane is 0. The direction of the vector u is flipped by redefining the 2 point of the vector P_0 and P_1. A new vector, w is created from v_0 to P_0, by adding the vector w and a fraction of vector u would give the vector from v_0 to the point of intersection, (w+su). The intersection point can be obtained by multiplying s into vector u after solving s in the dot product condition: n.(w+su)=0.

The calculation for the plane line intersection does not check whether the intersection point falls within the 60 cells. Another function was created to check if the intersection points falls within the cells using the coordinates of the 60 cells and intersection point. When the intersection points fall within any 60 of the 60 cells, that ray will be saved into an array. In cases where the intersection points fall within the module and not within the cells, it will be saved into another array for calculations of the rays that will be reflected internally in the module. The function works by checking whether the intersection point falls within any of the 4 corners of the 60 cells.

Rays that falls within the module but is not captured by the solar cells are not totally wasted, there is still a certain amount of ray that can be reflected to the cells from the front glass. . The first step is to find the intersection point of the ray and the front glass of the module which can be done by using the same method discussed in the previous section. For the ray to be reflected, the angle of incidence must be greater than the critical angle. The angle of incidence can be obtained by using equation (12), where $\bar{i}$ and $\bar{n}$ is the vector of the incident ray and the normal of the front glass respectively, while $|\bar{i}|$ and $|\bar{n}|$ is the magnitude of the vector.

$$incidence = \frac{180}{\pi}\left(cos^{-1} \times \frac{\bar{i}\,.\,\bar{n}}{|\bar{i}|.\,|\bar{n}|}\right) \qquad (12)$$

In the law of reflections, the angle of incidence is equal to the angle of reflection. The distance from reflected ray to the normal is the same as the distance from the incident ray to the normal. The distance between the incident ray and the normal can be calculated using dot product again. The line $(\bar{i}.\hat{n})\hat{n}$ is the projection of the incident ray in the direction of the normal. By subtracting $(\bar{i}.\hat{n})\hat{n}$ from vector i , the vector $\bar{i}-(\bar{i}.\hat{n})\hat{n}$ is formed. The vector $\bar{i}-(\bar{i}.\hat{n})\hat{n}$ is then multiplied by 2 to obtain the final position of the reflected ray. The same plane-line intersection and cell check function is then used again to find whether it falls within the cell. A separate array will be used to collect all the internally reflected rays that is captured by the cell.

Reflected lights that scatters in different directions have different intensity of its own, the intensity varies depending on the reflectivity of the surface it reflects on and the direction it scatters from the incident light. The irradiance, s(θ) of the scattered ray at certain direction can be calculated using the Equation (1) [20]. Where aue is the unit area of the ground, ∅p is the power of the incident light, WARg is the weighted average reflectance of the ground and sn(θ) is the measured normalized radiant intensity of the ground.

$$s(\theta) = aue.\emptyset p.(WARg)\frac{sn(\theta)}{\iint sn(\theta)\,sind\varphi d\theta} \qquad (13)$$

All the captured rays are tagged to a specific irradiance which will then be summed up to get the total power gain from the rear using equation (15). Where the irradiance of a ray is multiplied with T1, which is the check function against the 60 cells, if the ray is captured T1 will be 1 if not it will be 0.

$$P_{total\,rear} = \int_y^y \int_x^x \int_\varphi^\varphi \int_\theta^\theta s(\theta).T1.(cell_1,.,cell_{60})d\varphi d\theta dxdy \qquad (14)$$

III. Results and Discussions

A simulation was done to understand the influence of ground reflectance directly under the module to the module current. Discrete points directly under the cells gaps of the module will be simulated per configuration, the gain of the 9 points will then be summed up as the total rear gain for that configuration. Due to the lack of computational resource, only 9 points around the module was simulated, with 5 points within the cell gap of the module, 2 points at the edge of the module and the last 2 points at 1m away from the edge of the module.

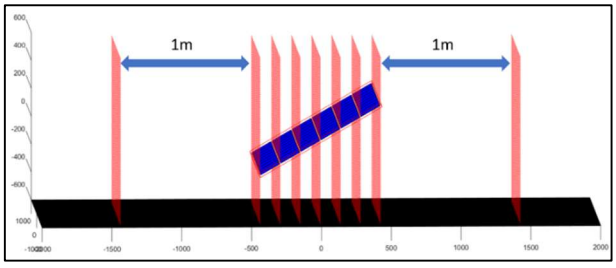

Figure 6. Areas simulated around the module

The total rear gain of all the configuration experimented were gathered and plotted into a graph, it is observed that the gain of the module decreases as the tilt angle and height increases.

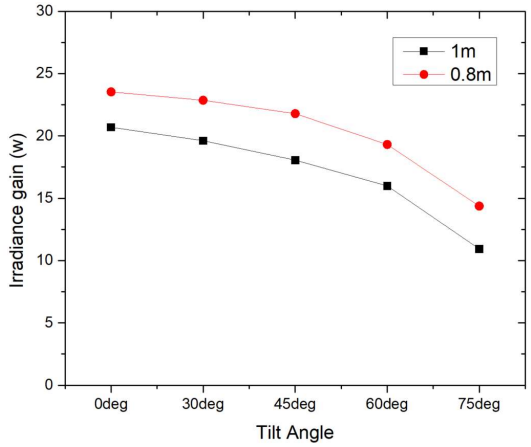

Figure 7. Rear irradiance gain per tilt angle

To graphically demonstrate the simulation results, 900 rays were simulated to scatter from ground, in the middle of the module of the figure below.

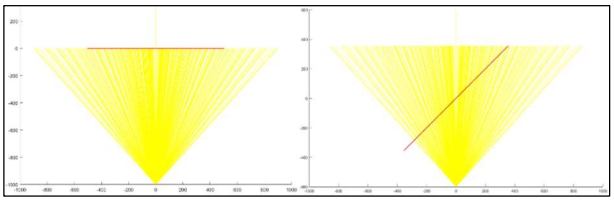

Figure 8. Side vide of module showing range of rays entering

As the height of the module increases, the amount of ray that can be captured by the module decreases. This is largely due to the fixed resolution of the scattered rays, thus distance between each ray increases as they travel further from the ground. The effect of the tilt angle on the gain is exponential and will only have big impact on the gain when is close to 90˚. Due to the distribution of light intensity, the scattered rays that are closer to the incident ray will have the higher irradiance compared to those that scatter away further from the incident ray.

Ground reflected rays that are reflected from areas outside of the module may not be captured at the rear of the module. It is observed that at certain distance, the reflected rays will start to fall on front surface instead of the rear.

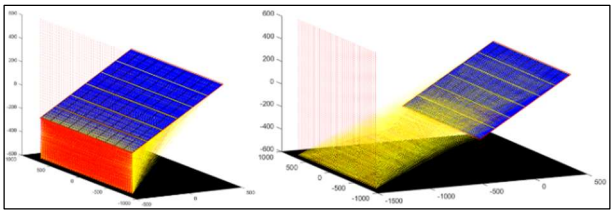

Figure 9. Rays reflecting onto the front of modules when distance from increases

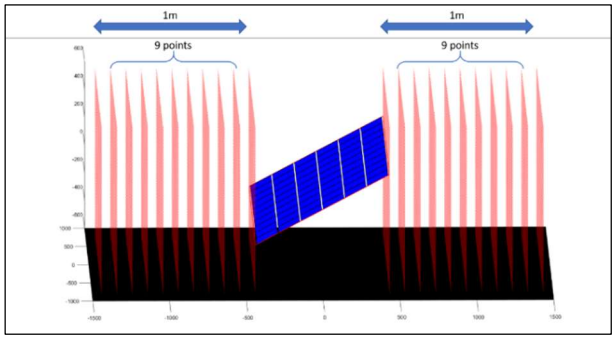

Figure 10. Rear irradiance gain per tilt angle

Ground reflected irradiance contributes strongly to the rear side irradiance gain at low tilt angle and with the increase of tilt angle the contributions reduce. While only bifacial modules have rear side irradiance gain from ground reflected rays, those rays that were reflected to the front side of the module contributes to front side irradiance gain of both bifacial and monofacial modules. Hence in this section the comparison of bifacial and monofacial modules the irradiance gains on both the rear and front side from the ground reflected rays and is discussed. As photovoltaics modules are mounted in an array, ground reflected ray from the array to array gap of 1m on both side of the module is taken in consideration. An additional 9 points within the 1m range from the edge of the module was simulated on both sides.

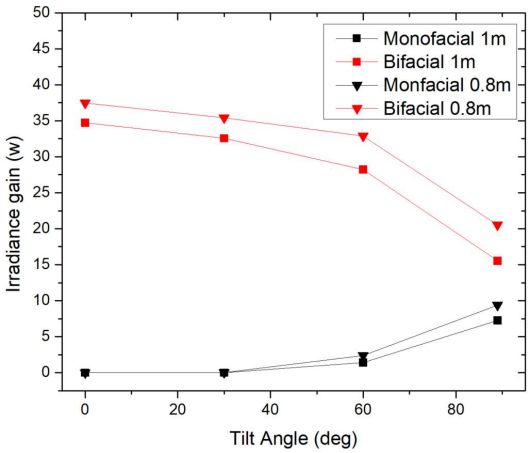

Figure 11. Irradiance gain per tilt angle for monofacial and bifacial modules

The simulated irradiance gain for bifacial module and monofacial was plotted in Figure 11. At 90° bifacial modules has twice the total irradiance gain as monofacial modules as both side of the module are absorption the irradiance. As the module tile angle reduces from 90° to 0° the total irradiance gains for bifacial modules increase with the increasing rear irradiance gain. While the front irradiance gain reduced for both bifacial and monofacial modules. When the tilt angle is less than 45°, there is zero irradiance gain from ground reflected irradiance for to the front side of the modules. Likewise, to the bifacial module with a lower mounting height of 0.8m from 1m at 90° the monofacial module had a ~30% increase in irradiance gain.

As the height of the module increases, the amount of ray that can be captured by the module decreases. This is largely due to the fixed resolution of the scattered rays, thus distance between each ray increases as they travel further from the ground. The effect of the tilt angle on the gain is exponential and will only have big impact on the gain when is close to 90˚. Due to the distribution of light intensity, the scattered rays that are closer to the incident ray will have the higher irradiance compared to those that scatter away further from the incident ray.

To further understand the effect of ground reflected irradiance to the front of the module, each unit of ground reflected rays were plotted in Figure 20 and Figure 21 for modules mounted at a height of 1m.

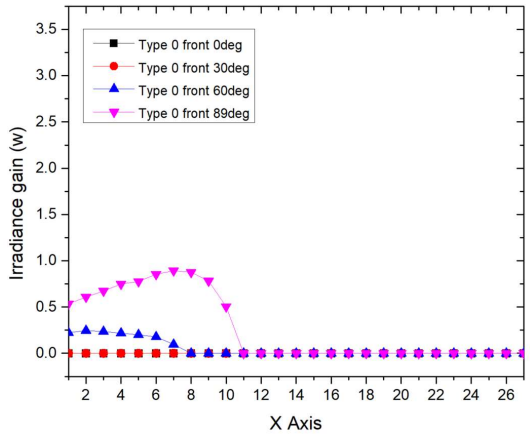

Figure 12. Front irradiance gain from ground reflected rays

The highest contribution to rear current at low tilt angle are those irradiances transmitted through the inter cell gap and reflected directly under the module from point 12 to 16 along the X axis. As the tilt angle increase, contributions of rear irradiance gain from ground directly under the module plotted as point 14 on the X axis reduces by 98% from 0° to 90°. The rear irradiance gain contribution from ground beyond the module increases by 121% at point 27.

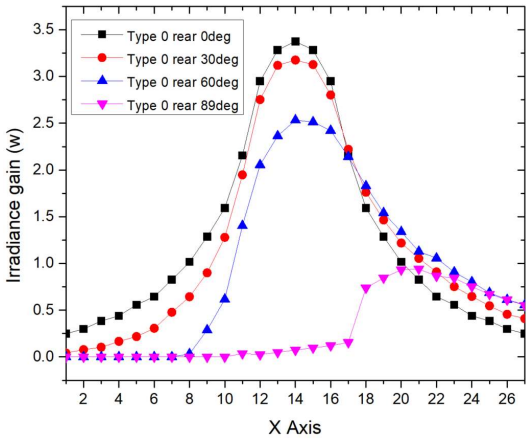

Figure 13. Rear irradiance gain from ground reflected rays

However, from Figure 13 the rear irradiance gain contribution from the edge most point is 92% lesser than middle point directly under the module. This phenomenon resulted in the reduction in irradiance gain shown in Figure 11 with increasing tilt angle. While the decrease in irradiance gain from points directly under the module with increasing tilt angle is sizeable, the slight increase in front irradiance gain from ground reflected irradiance which increasing tilt angle as plotted in Figure 20 thus reducing the total irradiance gain for bifacial modules at increasing tilt angles.

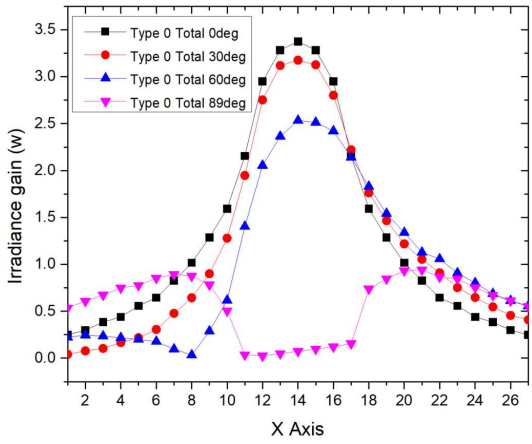

Figure 14. Total irradiance gain for bifacial modules from ground reflected rays

The main irradiance gain for bifacial modules are from the reflected rays directly under the module. This rear side gain is most significant at low modules tilt angle near 0°. Comparing additional ground reflected irradiance gained with the front side direct irradiance on the module front, the net gain for Type 0 bifacial modules mounted at a tilt angle of 0° at 1m height with an array to array distant of 1m over monofacial modules is ~ 27%. With the increase in tilt angle from 0° to 90°, the net gain increases sharply to 29%, 44% and 688% at 30°, 60°, and 90° respectively due to the sharp reduction of direct front side with increasing tilt angle.

The comparison could be done between bifacial the monofacial modules mounted at the same varying tilt angles for technical understanding, but seldom are monofacial mounted at an angle as it is the most optimal mounted perpendicular to the direct irradiance at 0°. Therefore, if we compare the bifacial module additional irradiance gain from ground reflected irradiance and a monofacial module with its mounting configuration optimized the net gain for bifacial modules reduces from 27% at 0° to 25%, 22%, and 12% at 30°, 60°, and 90° respectively. From these simulations the optimal tilt angle for both bifacial and monofacial modules are both at 0°. Similarly, to the tilt angle, to capture the most ground reflected irradiance the module should be closer to the ground. As there are associated overheating risk with the lack of module ground clearance with loss in performance, and the addition gain in reduced mounting height is minimal as compared to tilt angle hence it would be prudent to optimize the bifacial mount to 0° tilt angle with minimum manufacturer recommended ground clearance.

IV. Conclusion

In this project, MATLAB model was created to simulate Bifacial Panels. This model propagates the light rays reflected by the ground into 1800 discrete vectors. To quantify the ground reflected rays' contribution to the rear side current, the intersection points of each reflected ray vectors to the module plane were calculated against the 60 cells within the module.

In addition to the ground reflected ray to the rear current, some rays might be transmitted through the cell gap. Those reflected rays that falls within the cell gap and with incoming angle greater than the critical angle of the front glass/air interface were calculated for second position after being reflected onto the front of the cells. The reflected vectors will be used to calculate and checked for intersection points against the 60 cells positions for internal gain calculation.

Adding on to the rays that are reflected directly under the module and the internally reflected rays, the model was also able to calculate the distance at which the reflected rays start to fall onto the front side of the module, the distance for the reflected rays to start falling on the front of the module is shown to be proportional to the height and tilt of the module. This calculation of the front gain can also be used on the Monofacial modules and to create more possibilities for bifacial modules to potentially increase its output.

Firstly, from the simulation done on varying tilt angle for Type 0 bifacial modules. The rear irradiance gain is a strong function of tilt angle. The main contributor of rear irradiance gain was identified to be reflected rays originating from directly under the module. Due to the reduction in cross section along the X-Z axis with increased tilt angle the ground reflected rays are not collected by rear of the module. At 0° the module area is 1.6m in Y axis and 1m in X thus a $1.6m^2$ collection surface. With the module tilted at 75° the effective collection surface drops by 77% to $0.36m^2$.

Secondly, across all tilt angle the irradiance gain for bifacial modules are significantly higher than monofacial module due to the addition irradiance gain from the rear. Like monofacial modules, bifacial modules could also absorb the additional irradiance gain from the front side of the module. The net gain for Type 0 bifacial modules mounted at a tilt angle of 0° at 1m hight with an array to array distant of 1m over monofacial modules is ~ 27%. With the increase in tilt angle from 0° to 90°, the net gain increases sharply to 29%, 44% and 688% at 30°, 60°, and 90° respectively due to the sharp reduction of direct front side with increasing tilt angle. seldom are monofacial mounted at an angle as it is the most optimal mounted perpendicular to the direct irradiance at 0°. Therefore, if we compare the bifacial module additional irradiance gain from ground reflected irradiance and a monofacial module with its mounting configuration optimized the net gain for bifacial modules reduces from 27% at 0° to 25%, 22%, and 12% at 30°, 60°, and 90° respectively. From these simulations the optimal tilt angle for both Type 0 bifacial and monofacial modules are both at 0°. Similarly, to the tilt angle, to capture the most ground reflected irradiance the module should be closer to the ground.

This project is still at initial stage where many other factors can still be added to improve the accuracy of the results to be useful to the module design and installation industry for improving the energy yield from Bifacial solar modules.

References

[1] Singh, G., 2013. Solar power generation by PV (photovoltaic) technology: A review. Energy, 53, pp.1-13

[2] Guerrero-Lemus, R., Vega, R., Kim, T., Kimm, A. and Shephard, L., 2016. Bifacial solar photovoltaics – A technology review. Renewable and Sustainable Energy Reviews, 60, pp.1533-1549.

[3] Razongles, G., Sicot, L., Joanny, M., Gerritsen, E., Lefillastre, P., Schroder, S. and Lay, P., 2016. Bifacial Photovoltaic Modules: Measurement Challenges. Energy Procedia, 92, pp.188-198

[4] Liliana, E. P. Yoewono and R. Intan, "Transparency modeling for mesh object using ray tracing," 2016 International Electronics Symposium (IES), Denpasar, 2016, pp. 385-388.

[5] Berrian, D., Libal, J., Klenk, M., Nussbaumer, H. and Kopecek, R., 2019. Performance of Bifacial PV Arrays With Fixed Tilt and Horizontal Single-Axis Tracking: Comparison of Simulated and Measured Data. IEEE Journal of Photovoltaics, 9(6), pp.1583-1589.

[6] J. P. Singh, S. Guo, I. M. Peters, A. G. Aberle and T. M. Walsh, "Comparison of Glass/Glass and Glass/Backsheet PV Modules Using Bifacial Silicon Solar Cells," in IEEE Journal of Photovoltaics, vol. 5, no. 3, pp. 783-791, May 2015.

[7] Sng, E., Sahadevan, A., C.D, S., Rohini, S., Malar, K., Roy, S. and Li Hong Lim, I., 2019. 4AV.1.12 Optimisation of Bifacial Photovoltics Module with Reflective Layer in Outdoor Performance.

[8] A. Asgharzadeh et al., "Analysis of the Impact of Installation Parameters and System Size on Bifacial Gain and Energy Yield of PV Systems," 2017 IEEE 44th Photovoltaic Specialist Conference (PVSC), Washington, DC, 2017, pp. 3333-3338.

[9] C. W. Hansen et al., "A Detailed Model of Rear-Side Irradiance for Bifacial PV Modules," 2017 IEEE 44th Photovoltaic Specialist Conference (PVSC), Washington, DC, 2017, pp. 1543-1548.

[10] C. W. Hansen et al., "Analysis of irradiance models for bifacial PV modules," 2016 IEEE 43rd Photovoltaic Specialists Conference (PVSC), Portland, OR, 2016, pp. 0138-0143.

[11] Guo, S., Schneider, J., Lu, F., Hanifi, H., Turek, M., Dyrba, M. and Peters, I., 2015. Investigation of the short-circuit current increase for PV modules using halved silicon wafer solar cells. Solar Energy Materials and Solar Cells, 133, pp.240-247.

[12] O'Rourke, Computational Geometry in C. Cambridge University Press, 1998